Dissimilarity Between Heat and Momentum Transfer of Turbulent Heat Transfer over Surfaces with Hemisphere Protrusions

Dissimilarity between heat and momentum transfer of turbulent heat transfer over surfaces with hemisphere protrusions

Rika Nagura, Yusuke Kuwata and Kazuhiko Suga

Abstract To explore how the roughness arrangement affects the turbulent heat transfer, direct numerical simulations of turbulent heat transfer over walls with regularly distributing hemisphere protrusions were performed by the lattice Boltzmann method. The friction Reynolds number was fixed at 660 and the fluid Prandtl number was 0.71 assuming an air flow. The roughness increases the momentum transfer more than the heat transfer. The Reynolds analogy factor, which measures the dissimilarity between the momentum and heat transfer, can be expressed as a function of the skin friction coefficient, inner-scaled equivalent roughness, and Prandtl number regardless of the roughness arrangement.

1 Introduction

The heat transfer over a roughened wall is of great engineering interest because the presence of wall roughness leads to a considerable enhancement of momentum, mass, and heat transfer. As the wall roughness enhances turbulence, secondary or tertiary flow as well as flow mixing, artificial roughness is frequently created to increase the heat transfer performance of engineering devices, such as internal cooling inside turbine blades [1], solar thermal systems [2], and heat transfer pipes [3]. Hence, a great deal of effort has been made to understand the effects of the wall roughness on heat and momentum transfer.

With regard to the momentum transfer, wall roughness hardly affects the momentum transfer provided that the wall roughness is buried within the viscous sublayer but has a considerable impact when the wall roughness protrudes into the logarithmic layer. As a consequence of the enhancement of the momentum transfer, the skin friction coefficient at a rough surface increases resulting in a downward shift in

Rika Nagura, Yusuke Kuwata, Kazuhiko Suga
Department of Mechanical Engineering, Osaka Prefecture University, Sakai, Japan, e-mail: kuwata@me.osakafu-u.ac.jp

the inner-scaled mean velocity. It is well established that the downward shift in the mean velocity profile, which is referred to as the velocity roughness function, can be expressed as a function of the inner-scaled equivalent roughness [4].

As for the effects on the heat transfer, wall roughness also leads to a downward shift in the inner-scaled mean temperature profiles due to an increase in the heat transfer over a rough surface. However, as the Reynolds analogy does no longer hold for rough wall turbulence, the temperature roughness function, which is a downward shift in the inner-scaled mean temperature profile, is lower than the velocity roughness function even though the Prandtl number is unity. There is still much controversy about the effects of wall roughness on the dissimilarity between the heat and momentum transfer and no universally-accepted correlation that can accurately predict the heat transfer rate over a rough surface. In this study, for the improvement of the prediction of turbulent heat transfer over a rough surface, we investigate the effects of the roughness arrangement on the dissimilarity between the heat and momentum transfer by means of direct numerical simulations (DNSs) of the turbulent heat transfer over surfaces with hemisphere protrusions.

2 Flow conditions

A schematic of a rough-walled open-channel flow is shown in Figure 1. Periodic boundary conditions were applied to the streamwise (x) and spanwise (z) directions, whereas a slip wall was considered for the top wall. The bottom wall was roughened by regularly distributing hemisphere protrusions with relatively large size of $k = 0.3L_y$, where L_y is the open-channel height. The distances between two neighboring hemispheres in the streamwise and spanwise directions (p_x and p_z, respectively) were systematically varied with the roughness density being fixed as shown in Figure 1. The rough surface is named NXMZ, where $N = p_x/k$ and $M = p_z/k$ stand for the streamwise and spanwise hemisphere pitches, respectively. The surface for case 20X2.5Z in Figure 1(a) has the smallest spanwise pitch of $p_z = 2.5k$ yielding the largest streamwise frontal area, whereas the surface for case 2.5X20Z in Figure 1(d) has the smallest frontal area. The streamwise and spanwise computational domain size were respectively $L_x = 6L_y$ and $L_z = 3L_y$ for cases 20X2.5Z, 10X5Z, and 5X10Z, but extended to 6δ in the spanwise direction for case 2.5X20Z. A flow was driven by a constant streamwise pressure difference, and the friction Reynolds number was fixed at $Re_\tau = 660$. The fluid Prandtl number was $Pr = 0.71$ assuming an air flow.

The flow field was simulated by the D3Q27 multiple-relaxation-time lattice Boltzmann method (LBM) [5], whereas we used D3Q19 regularized LBM [6] for the scaler field. The computational grid was uniform with equal spacing in all directions, and the grid points across the half channel height were 270 such that the resolution in wall units is comparable to those used in the lattice Boltzmann DNS studies [7].

3 Results and discussion

The modification of the mean velocity and temperature profiles are presented in Figure 2, where the superficial $x-z$ plane-averaged inner-scaled streamwise mean velocity $\overline{u}^+$ and mean temperature $\overline{\theta}^+$ are shown against the inner-scaled effective wall-normal distance y_e^+. Here, θ indicates the fluid temperature T minus the wall temperature T_w: $\theta = T - T_w$, and the effective wall-normal distance y_e is defined as the wall-normal integral of the $x-z$ plane porosity: $y_e = \int_0^y \varphi dy$, which accounts for a virtual origin of a rough wall [7]. The figure confirms that the $\overline{u}^+$ and $\overline{\theta}^+$ profiles for rough wall cases are shifted downward. The hemisphere arrangement affects the $\overline{u}^+$ profiles considerably, whereas the $\overline{\theta}^+$ profiles remain almost unaffected. The downward shift in $\overline{u}^+$ is the largest for case 20X2.5Z, followed by 10X5Z, 5X10Z, and 2.5X10Z.

To better understand the behaviors of the downward shift values, the velocity and temperature roughness functions (ΔU^+ and $\Delta\Theta^+$, respectively) are plotted against equivalent roughness height k_s^+ in Figure 3. For comparison, the DNS data for the sinusoidal roughness from [10] and grid-blasted surface from [9] are also shown.

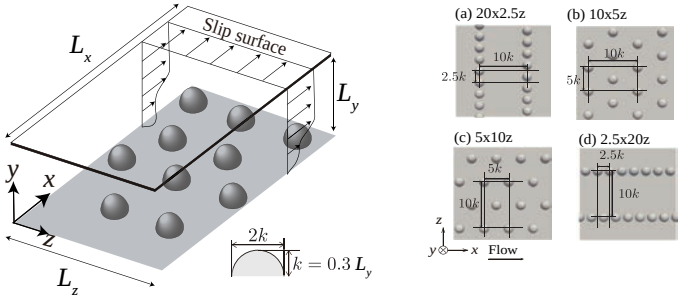

Fig. 1 Computational geometry of a rough-walled open channel flow.

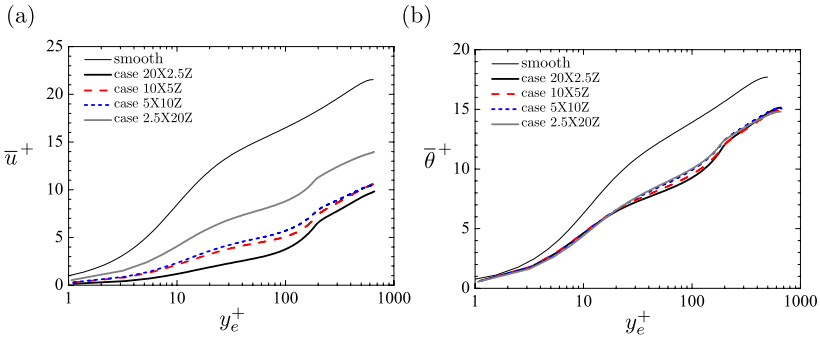

Fig. 2 (a)Inner-scaled streamwise mean velocity profiles, (b) Inner-scaled mean temperature profiles. The DNS data from [8] is also included.

Here, ΔU^+ ($\Delta\Theta^+$) is defined as a mean difference in the $\overline{u}^+$ ($\overline{\theta}^+$) profile between the smooth wall and rough wall cases in $k < y < \delta$. The trend of $\Delta\Theta^+$ against k_s^+ is found to be very different from that of ΔU^+: ΔU^+ monotonically increases with k_s^+, whereas $\Delta\Theta^+$ for the present results exhibits an almost constant value of $\Delta\Theta \simeq 3$ despite the considerable difference in the hemisphere arrangement. This plateau value is seemed to be somewhat smaller than those for the sinusoidal roughness and grid-blasted surface, indicating that the heat transfer enhancement relative to the momentum transfer enhancement is smaller for the present rough surfaces. The possible explanation is that the present rough surfaces tend to yield larger pressure drag which increases the momentum transfer but not the heat transfer. It is well established that ΔU^+ against k_s^+ collapses onto a single curve irrespective of the surface texture in the fully rough regime; however, $\Delta\Theta^+$ against k_s^+ is found to be rather scattered, indicating that $\Delta\Theta^+$ is not expressed as a function of k_s^+ solely but other roughness or flow parameters should be taken into account.

To quantify the augmentation of the heat and momentum transfer, the skin friction coefficient C_f and Stanton number St normalized by the corresponding values C_{f0} and St_0 for smooth wall turbulence are shown in Figure 4. Note that C_f and St are the averaged values over the rough surfaces. For a better physical understanding, C_f is decomposed into the contribution by the pressure and viscous effects. It is clear that the augmentation of C_f can be attributed to the role of the pressure, and the contribution by the pressure largely depends on the hemisphere arrangement. On the other hand, although St is also enhanced by the wall roughness, the augmentation of St is much smaller than that of C_f, which is considered to be due to an absence of the pressure term in the energy equation. Both C_f and St show the largest values for case 20X2.5Z where the streamwise frontal area is the largest, whereas the case with streamwise aligned roughness elements (case 2.5X20Z) results in the smallest C_f and St values.

Finally, to explore the predictive method for the dissimilarity between the momentum and heat transfer, we discuss the Reynolds analogy factor, which is defined as the ratio of the doubled Stanton number to the Skin friction coefficient: $RA = 2St/C_f$. When the heat transfer exceeds the momentum transfer, the RA value is greater than unity, whereas it is less than unity in the opposite situation. Figure 5 presents the Reynolds analogy factor RA normalized by a corresponding value for smooth wall turbulence RA_0, together with the correlation proposed by [12]:

$$RA/RA_0 = \frac{Pr^{2/3}}{1 + \sqrt{0.5C_f}\left(5.19(k_s^+)^{0.2}Pr^{0.44} - 8.5\right)}, \tag{1}$$

and that by [11],

$$RA/RA_0 = \frac{Pr^{2/3}}{Pr_t + \sqrt{0.5C_f}\left((k_s^+)^{0.2}Pr^{0.44}/C\right)}. \tag{2}$$

where the turbulent Prandtl number is assumed to be unity, $Pr_t = 1$, and the model constant of $C = 0.35$ is assigned [13]. The figure demonstrates that the RA values

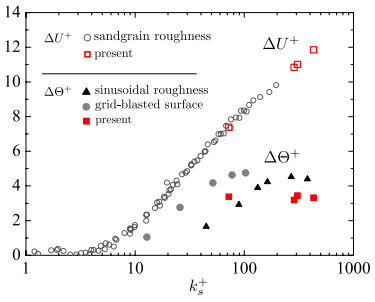

Fig. 3 Velocity and temperature roughness function against the inner-scaled equivalent roughness. The experimental data from [14], and the DNS data for sinusoidal roughness from [10] and grid-blasted surface from [9] are shown.

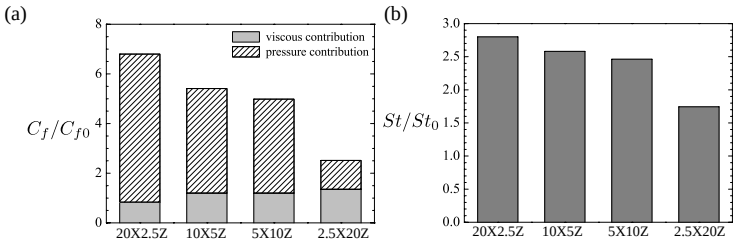

Fig. 4 (a) augmentation of the skin friction coefficient C_f/C_{f0} and (b) augmentation of the Stanton number St/St_0.

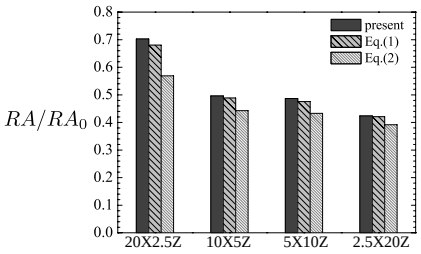

Fig. 5 Comparison of the Reynolds analogy factor normalized by the smooth wall value RA/RA_0.

predicted by the Eqs. (1) and (2) are lower than unity, suggesting that both of the models reproduce the dissimilar trend between the heat and momentum transfer. In particular, the correlation by [12] gives solutions that are significantly closer to the present DNS results. This suggests that the Reynolds analogy factor, which measures the dissimilarity between the heat and momentum transfer, can be expressed as a function of the skin friction coefficient, Prandtl number, and the inner-scaled equivalent roughness, irrespective of the roughness arrangement.

4 Conclusion

Direct numerical simulations of turbulent heat transfer over walls with regularly distributing hemisphere protrusions is performed to get insight into how the roughness

arrangement affects the turbulent heat transfer. The roughness arrangement largely affects the momentum and heat transfer: the augmentation of the momentum and heat transfer is the largest for the surface with the maximum streamwise frontal area, whereas it is the smallest for the streamwise-aligned hemisphere protrusions. As the hemisphere protrusions particularly increases pressure drag, the roughness increases the momentum transfer more than the heat transfer, resulting in the dissimilarity between the momentum and heat transfer. The Reynolds analogy factor can be expressed as a function of the skin friction coefficient, inner-scaled equivalent roughness, and Prandtl number regardless of the roughness arrangement.

Acknowledgements A part of this study was financially supported by JSPS Japan (No.17K1459) and the Research Association of Automotive Internal Combustion Engines. The numerical calculations were carried out on the TSUBAME3.0 supercomputer at Tokyo Institute of Technology.

References

1. A. Murata and S. Mochizuki (2001) Comparison between laminar and turbulent heat transfer in a stationary square duct with transverse or angled rib turbulators, *International Journal of Heat and Mass Transfer, vol. 44 (6), pp. 1127-1141*
2. S. Chamoli, N.S. Thakur, and J.S. Saini (2012) A review of turbulence promoters used in solar thermal systems, *Renewable and Sustainable Energy Reviews, vol.16(5), pp.3154-3175*
3. K. Akermann, P. Renze, J. Dietl, and W. Schröder (2020) Large-Eddy Simulation of turbulent heat transfer in a multiple-started helically rib-roughened pipe, *International Journal of Heat and Mass Transfer, vol. 154, pp. 119667*
4. K.A. Flack and M.P. Schultz (2010) Review of hydraulic roughness scales in the fully rough regime, *Journal of Fluids Engineering 132.4*
5. K. Suga, Y. Kuwata, K. Takashima and R. Chikasue (2015) A D3Q27 multiple-relaxation-time lattice Boltzmann method for tuebulent flows, *Computers & Mathematics with Applications, vol. 69, pp. 518-529*
6. K. Suga, R. Chikasue and Y. Kuwata (2017) Modelling turbulent and dispersion heat fluxes in turbulent porous medium flows using the resolved LES data, *International Journal of Heat and Fluid Flow, vol. 68, pp. 225-236*
7. Y. Kuwata and Y. Kawaguchi (2019) Direct numerical simulation of turbulence over systematically varied irregular rough surfaces, *Journal of Fluid Mechanics, vol. 862, pp. 781-815*
8. F. Lluesma-Rodríguez, S. Hoyas, M. Perez-Quiles (2018) Influence of the computational domain on DNS of turbulent heat trabsfer up to $Re_\tau = 2000$ for $Pr = 0.71$, *International Journal of Heat and Mass Transfer, vol. 122, pp.983-992*
9. J. Peeters and N. Sandham (2019) Turbulent heat transfer in channels with irregular roughness, *International Journal of Heat and Mass Transfer, vol. 138, pp.454-467*
10. M. MacDonald, N. Hutchins and D. Chung (2018) Roughness effects in turbulent forced convection, *Journal of Fluid Mechanics, vol. 861, pp. 138-162*
11. W. Kays and M. Crawford (1993) *Convective Heat and Mass Transfer*, McGraw-Hill
12. D. Dipprey and R. Sabersky (1963) Heat and momentum transfer in smooth and rough tubes at various Prandtl numbers, *International Journal of Heat and Mass Transfer, vol. 6, pp. 329-353*
13. J. P. Bons (2002) St and Cf augmentation for real turbine roughness with elevated freestream turbulence, *Journal of Turbomachinery, vol. 124 (4), pp. 632-644*
14. J. Nikuradse (1933) Laws of flow in rough pipes, *in VDI Forschungsheft*